ARTICLE

Amitabha Chattopadhyay · Ajuna Arora
Devaki A. Kelkar

Dynamics of a membrane-bound tryptophan analog in environments of varying hydration: a fluorescence approach

Abstract Tryptophan octyl ester (TOE) represents an important model for membrane-bound tryptophan residues. In this article, we have employed a combination of wavelength-selective fluorescence and time-resolved fluorescence spectroscopies to monitor the effect of varying degrees of hydration on the dynamics of TOE in reverse micellar environments formed by sodium bis(2-ethylhexyl) sulfosuccinate (AOT) in isooctane. Our results show that TOE exhibits red edge excitation shift (REES) and other wavelength-selective fluorescence effects when bound to reverse micelles of AOT. Fluorescence parameters such as intensity, emission maximum, anisotropy, and lifetime of TOE in reverse micelles of AOT depend on [water]/[surfactant] molar ratio (w_o). These results are relevant and potentially useful for analyzing dynamics of proteins or peptides bound to membranes or membrane-mimetic media under conditions of changing hydration.

Introduction

Tryptophan is the most extensively used amino acid for fluorescence analysis of proteins. The role of tryptophan residues in the structure and function of membrane

A. Chattopadhyay (✉) · A. Arora
D. A. Kelkar
Centre for Cellular and Molecular Biology, Uppal Road,
Hyderabad 500 007, India
E-mail: amit@ccmb.res.in
Tel.: +91-40-27192578
Fax: +91-40-27160311

proteins and peptides has attracted considerable attention. Membrane-spanning proteins are reported to have a significantly higher tryptophan content than soluble proteins (Schiffer et al. 1992). In addition, it has been observed that tryptophan residues in integral membrane proteins and peptides are not uniformly distributed and that they tend to be localized toward the membrane interface. Statistical studies of sequence databases and available crystal structures of integral membrane proteins also show preferential clustering of tryptophan residues at the membrane interface (Reithmeier 1995; Ulmschneider and Sansom 2001). Furthermore, tryptophan has been found to be an efficient anchor at the membrane interface for transmembrane peptides and proteins (Schiffer et al. 1992) and defines the hydrophobic length of transmembrane helices (Demmers et al. 2001). The tryptophan-rich aromatic belt at the membrane interface in transmembrane helices is thought to stabilize the helix with respect to the membrane environment (Reithmeier 1995). Importantly, the role of tryptophan residues in maintaining the structure and function of membrane proteins is exemplified by the fact that substitution or deletion of tryptophans often results in reduction or loss of protein functionality (Becker et al. 1991; Miller and Falke 2004).

The analysis of fluorescence from multitryptophan proteins is often complicated because of the complexity of fluorescence processes in such systems and the heterogeneity in fluorescence parameters (such as quantum yield and lifetime) due to the environmental sensitivity of individual tryptophans. Use of suitable model systems could prove to be helpful in such cases. In spite of the importance of membrane-bound tryptophan residues very few model systems have been developed that could help understand the behavior of tryptophan residues in the membrane. Tryptophan octyl ester (TOE) has been recognized as an important model for membrane-bound tryptophan residues (see Fig. 1). The fluorescence characteristics of TOE incorporated into model membranes and membrane-mimetic systems have been shown to be similar to that of membrane-bound
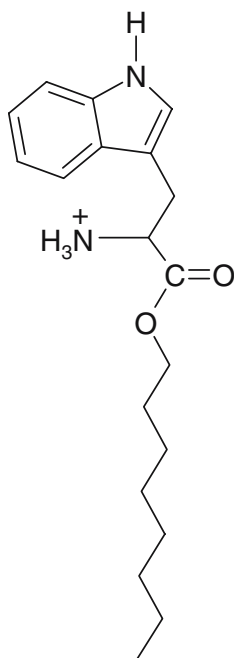
Fig. 1 Chemical structure of the protonated form of TOE. This form is predominant under conditions of the experiments described here (see "Materials and methods" and "Discussion" for details)

tryptophans (Ladokhin and Holloway 1995; Chattopadhyay et al. 1997; de Foresta et al. 1999; Sengupta and Sengupta 2000).

In this article, we have employed a combination of wavelength-selective fluorescence and time-resolved fluorescence spectroscopies to monitor the effect of varying degrees of hydration on the dynamics of TOE in reverse micellar environments formed by AOT [sodium bis(2-ethylhexyl) sulfosuccinate] in isooctane. Hydration is known to play a key role in lipid–protein interactions in membranes (Ho and Stubbs 1992). Reverse micelles offer the unique advantage of monitoring dynamics of embedded peptides and proteins with varying degrees of hydration, i.e., in a controlled water-restricted environment (Luisi and Magid 1986). They represent an attractive model system for biomembranes since they mimic a number of important and essential features of biological membranes although the constituent monomers in reverse micelles are negatively charged while in biomembranes the constituent lipids could be of various charge types.

Wavelength-selective fluorescence comprises a set of approaches based on the red edge effect in fluorescence spectroscopy, which can be used to directly monitor the environment and dynamics around a fluorophore in an organized molecular assembly (Chattopadhyay 2003). A shift in the wavelength of maximum fluorescence emission toward higher wavelengths, caused by a shift in the excitation wavelength toward the red edge of absorption band, is termed red edge excitation shift (REES). This effect is mostly observed with polar fluorophores in motionally restricted media such as very viscous

solutions or condensed phases where the dipolar relaxation time for the solvent shell around a fluorophore is comparable to or longer than its fluorescence lifetime. The unique feature of REES is that while other fluorescence techniques yield information about the fluorophore itself, REES provides information about the relative rates of solvent relaxation which is not possible to obtain by other techniques. We have previously shown that REES and related techniques (wavelength-selective fluorescence approach) serve as powerful tools to monitor the organization and dynamics of probes and peptides bound to membranes and membrane-mimetic media such as micelles and reverse micelles (reviewed in Chattopadhyay 2003; Raghuraman et al. 2005).

Materials and methods

Materials

AOT and TOE were purchased from Sigma Chemical Co. (St Louis, MO, USA). The purity of AOT was confirmed by the good agreement of its UV absorption spectrum with previously reported spectrum (Luisi and Magid 1986). The purity of TOE was confirmed as previously reported (Chattopadhyay et al. 1997) by thin layer chromatography on precoated silica gel plates in n-hexane/methanol/diethyl ether/acetic acid (80:25:20:1, v/v/v/v), which gave a single spot with both ninhydrin and Ehrlich spray. The isooctane used was of spectroscopic grade. Water was purified through a Millipore (Bedford, MA, USA) Milli-Q system and used throughout.

Preparation of reverse micelles

Reverse micelles of AOT-containing TOE were prepared without the addition of any cosolvent as described earlier (Chattopadhyay et al. 2002). Briefly, TOE in methanol was dried under a stream of nitrogen while being warmed gently (~35°C). After further drying under high vacuum for at least 4 h, 1.5 ml of 25 mM AOT in isooctane was added, and the samples were vortexed for 3 min. Appropriate amounts of water were subsequently added to make reverse micellar dispersions of different [water]/[surfactant] molar ratio (w_o). Background samples were prepared the same way except that TOE was not added to them. Samples were kept in the dark for at least 8 h before measuring fluorescence. All experiments were done at 23°C.

The molar ratio of fluorophore (TOE) to surfactant (AOT) was carefully chosen to give an optimum signal-to-noise ratio with minimal perturbation to the micellar organization and negligible interprobe interactions. The concentration of TOE used for experiments in which fluorescence intensity and anisotropy were measured was 20 μM, while for REES and time-resolved fluorescence experiments, it was 100 and 50 μM, respectively.

The concentration of AOT was 25 mM in all cases which is much above the critical micelle concentration of AOT in isooctane (Mukherjee et al. 1993), thereby ensuring that it is in the reverse micellar form. This corresponds to a fluorophore-to-surfactant molar ratio of not more than 1:250 (mol/mol) in any case. At such a fluorophore-to-surfactant ratio, not more than one probe molecule would be present per reverse micelle on an average, keeping in mind the aggregation number of AOT (Zhou et al. 2002), thereby ruling out any probe aggregation effects.

Steady-state fluorescence measurements

Steady-state fluorescence measurements were performed with a Hitachi F-4010 spectrofluorometer using 1 cm path length quartz cuvettes. For REES experiments, 1 cm path length quartz cuvettes (Hellma, Germany) which are mirror-coated on two surfaces were used for enhancing the signal-to-noise ratio. Excitation and emission slits with a nominal band pass of 5 nm were used for all measurements. Background intensities of samples in which the fluorophore (TOE) was omitted were negligible in most cases and were subtracted from each sample spectrum to cancel out any contribution due to the solvent Raman peak and other scattering artifacts. The spectral shifts obtained with different sets of samples were identical in most cases. In other cases, the values were within ± 1 nm of the ones reported. Fluorescence anisotropy measurements were performed using a Hitachi polarization accessory. Anisotropy values were calculated from the equation (Lakowicz 1999):

$$r = (I_{VV} - GI_{VH})/(I_{VV} + 2GI_{VH}) \qquad (1)$$

where I_{VV} and I_{VH} are the measured fluorescence intensities (after appropriate background subtraction) with the excitation polarizer vertically oriented and emission polarizer vertically and horizontally oriented, respectively. G, the grating correction factor, is the ratio of the efficiencies of the detection system for vertically and horizontally polarized lights and is equal to I_{HV}/I_{HH}. All the experiments were done with multiple sets of samples and average values of anisotropy are shown in Figs. 4 and 5.

Time-resolved fluorescence measurements

Fluorescence lifetimes were calculated from time-resolved fluorescence intensity decays using a Photon Technology International (London, Western Ontario, Canada) LS-100 luminescence spectrophotometer in the time-correlated single photon counting mode. This machine uses a thyratron-gated nanosecond flash lamp filled with nitrogen as the plasma gas (17 ± 1 in. mercury vacuum) and is run at 17–20 kHz. Lamp profiles were measured at the excitation wavelength using Ludox (colloidal silica) as the scatterer. To optimize the signal-to-noise ratio, 10,000 photon counts were collected in the peak channel. The excitation wavelength used was 297 nm and emission was set at 328 nm. All the experiments were performed using excitation and emission slits with a band pass of 10 nm or less. The sample and the scatterer were alternated after every 5% acquisition (which amounts to ~1 min for a typical 20 min total acquisition time) to ensure compensation for shape and timing drifts occurring during the period of data collection. This arrangement also prevents any prolonged exposure of the sample to the excitation beam, thereby avoiding any possible photo damage to the fluorophore. The data stored in a multichannel analyzer were routinely transferred to an IBM PC for analysis. Fluorescence intensity decay curves so obtained were deconvoluted with the instrument response function and analyzed as a sum of exponential terms:

$$F(t) = \Sigma_i \alpha_i \exp(-t/\tau_i) \qquad (2)$$

where $F(t)$ is the fluorescence intensity at time t and α_i is a pre-exponential factor representing the fractional contribution to the time-resolved decay of the component with a lifetime τ_i such that $\Sigma_i \alpha_i = 1$. The decay parameters were recovered using a nonlinear least squares iterative fitting procedure based on the Marquardt algorithm (Bevington 1969). The program also includes statistical and plotting subroutine packages (O'Connor and Phillips 1984). The goodness of fit of a given set of observed data and the chosen function was evaluated by the reduced χ^2 ratio, the weighted residuals (Lampert et al. 1983), and the autocorrelation function of the weighted residuals (Grinvald and Steinberg 1974). A fit was considered acceptable when plots of the weighted residuals and the autocorrelation function showed random deviation about zero with a minimum χ^2 value not more than 1.4. Mean (average) lifetimes $<\tau>$ for biexponential decays of fluorescence were calculated from the decay times and pre-exponential factors using the following equation (Lakowicz 1999):

$$<\tau> = (\alpha_1 \tau_1^2 + \alpha_2 \tau_2^2)/(\alpha_1 \tau_1 + \alpha_2 \tau_2) \qquad (3)$$

Results

The fluorescence emission spectra and intensity of TOE incorporated in AOT reverse micelles as a function of w_o are shown in Fig. 2. Figure 2a shows that the maximum fluorescence emission of TOE in AOT reverse micelles without any added water ($w_o = 0$) is 324 nm, which is significantly blue-shifted relative to the emission maximum in aqueous buffer at pH 7 (~353 nm) or in membranes (~335 nm; Chattopadhyay et al. 1997). This blue shift in emission maximum indicates the nonpolar nature of the site of localization of the tryptophan moiety on TOE in the reverse micellar assembly. However, the fluorescence emission maximum of TOE undergoes a
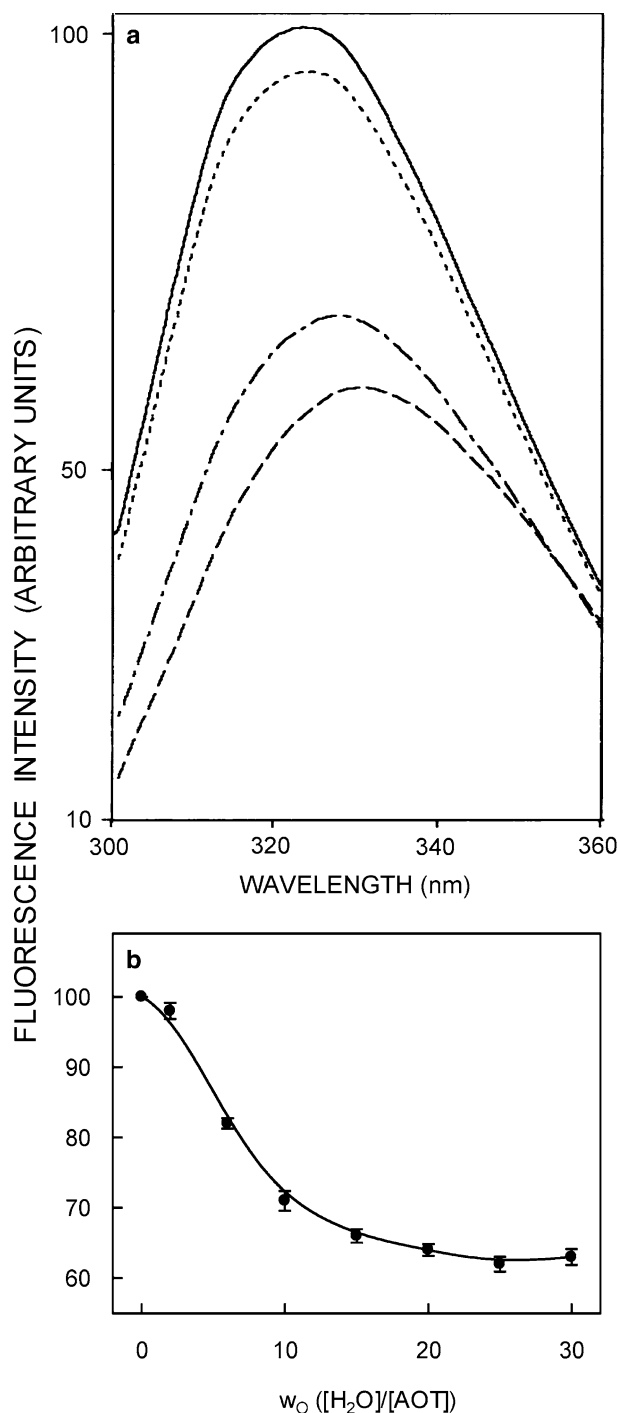
‌

Fig. 2 Effect of increasing amounts of added water on (**a**) fluorescence emission spectra and (**b**) fluorescence intensity of TOE in AOT reverse micelles. Fluorescence emission spectra are shown as a function of [water]/[surfactant] molar ratio (w_o) in order of decreasing intensity corresponding to $w_o = 0$ (*solid line*), 4 (*dotted line*), 10 (*dashed dotted line*), and 20 (*broken line*). Fluorescence intensity was monitored at 328 nm and plotted as a function of w_o in (**b**). The data points shown are the means ± standard errors of three independent measurements. The excitation wavelength used was 280 nm. The ratio of fluorophore (*TOE*) to surfactant (*AOT*) was 1:1250 (mol/mol). See "Materials and methods" for other details

progressive red shift of 10 nm (from 324 to 334 nm) when the water content is increased, i.e., when w_o is increased from 0 to 30 (Fig. 2a). This red shift in emission is accompanied with a marked reduction ($\sim 40\%$) in peak fluorescence intensity when w_o is increased from 0 to 30 (Fig. 2b). Taken together, these results clearly show that there is an increase in the polarity around the tryptophan of TOE in AOT reverse micelles due to an increase in water content, in agreement with an earlier report (Sengupta and Sengupta 2000).

The shifts in the maxima of fluorescence emission[1] of TOE in AOT reverse micelles of varying w_o as a function of excitation wavelength are shown in Fig. 3. As the excitation wavelength is changed from 280 to 302 nm, the emission maxima of TOE shift toward longer wavelengths in all cases. They are shifted from 324 to 329 nm (for $w_o = 0$), 325 to 330 ($w_o = 5$), 328 to 333 ($w_o = 10$), 332 to 337 ($w_o = 20$), 334 to 339 nm ($w_o = 30$), which correspond to a REES of 5 nm. A further red shift could be possible if excitation is carried out beyond 302 nm. We found it difficult to work in this wavelength range due to the low signal-to-noise ratio and artifacts due to the solvent Raman peak that sometimes remained even after background subtraction. Such dependence of the emission maximum on excitation wavelength is characteristic of the REES. This implies that the tryptophan moiety of TOE is localized in a motionally restricted region of the reverse micelle. We have previously shown that when bound to membranes, the tryptophan moiety of TOE is localized in a motionally restricted interfacial region of the membrane and exhibits REES (Chattopadhyay et al. 1997). Thus, the observation of REES for TOE bound to reverse micelles would directly imply that the interfacial region of the reverse micelle offers considerable restriction to the reorientational motion of the solvent molecules (dipoles) around the excited state fluorophore. The interfacial region of reverse micelles is associated with bound water with characteristic dynamics (Jain et al. 1989; Ikushima et al. 1997; Faeder and Ladanyi 2000; Brubach et al. 2001; Venables et al. 2001). Since REES arises due to the rate of reorientational motion of solvent molecules, these results therefore assume significance in the context of recent reports of slow ($\sim$ns) water relaxation in reverse micelles (Bhattacharyya 2003).

The steady-state anisotropy of TOE in AOT reverse micelles as a function of increasing amounts of water is shown in Fig. 4. As shown in the figure, fluorescence anisotropy of TOE decreases with increasing w_o, which implies that there is a decrease in rotational restriction experienced by the tryptophan moiety with increasing hydration. In addition to the shift in

---

[1]We have used the term maximum of fluorescence emission in a somewhat wider sense here. In every case, we have monitored the wavelength corresponding to maximum fluorescence intensity, as well as the center of mass of the fluorescence emission. In most cases, both these methods yielded the same wavelength. In cases where minor discrepancies were found, the center of mass of emission has been reported as the fluorescence maximum

emission maximum on red edge excitation, fluorescence anisotropy is also known to depend on the excitation wavelength in motionally restricted media (Mukherjee and Chattopadhyay 1995 and references therein). Due to strong dipolar interactions with the surrounding solvent molecules, there is a decreased rotational rate of the fluorophore in the solvent-relaxed state. Red edge excitation results in selective excitation of this subclass of fluorophore. Because of strong interactions with the polar solvent molecules in the excited state, one may expect these 'solvent-relaxed' fluorophores to rotate more slowly, thereby increasing the anisotropy. Figure 5a shows the fluorescence anisotropy of TOE in AOT reverse micelles of various w_o plotted as a function of excitation wavelength. The considerable increase in fluorescence anisotropy in all cases as the excitation wavelength is shifted toward the red edge reinforces our earlier conclusion that the tryptophan moiety is in a motionally restricted environment in the reverse micelle. Such an increase in anisotropy upon red edge excitation for peptides and proteins containing tryptophans, especially in media of reduced mobility, has been previously reported (Valeur and Weber 1977, 1978; Mukherjee and Chattopadhyay 1994).It should be noted that in agreement with Fig. 4, lower anisotropy values are displayed in general by samples with higher w_o.

It is known that tryptophan has two overlapping $S_o \rightarrow S_1$ electronic transitions (^1L_a and ^1L_b), which are almost perpendicular to each other (Callis 1997). Both $S_o \rightarrow {}^1L_a$ and $S_o \rightarrow {}^1L_b$ transitions occur in the 260–300 nm range. In nonpolar solvents, ^1L_a has higher energy than ^1L_b. However, in polar solvents, the energy level of ^1L_a is lowered, making it the lowest energy state. This inversion is believed to occur because ^1L_a transition has higher dipole moment (as it is directed through the ring –NH group) and can have dipole–dipole interactions with polar solvent molecules. Irrespective of whether ^1L_a or ^1L_b is the lowest S_1 state, equilibration between these two states is believed to be very fast (of the order of 10^{-12} s), so that only emission from the lower S_1 state is observed (Ruggiero et al. 1990). In a motionally restricted polar environment, absorption at the red edge photoselects the lowest energy S_1 (^1L_a in this case), and thus the anisotropy is high since depolarization only due to small angular differences between the absorption and emission transition moments and solvent reorientation, if any, occurs. Excitation at shorter wavelengths, however, populates both ^1L_a and ^1L_b states. Equilibration between these two states produces a depolarization due to the approximately 90° angular difference between ^1L_a and ^1L_b moments. Thus, near 285 nm, there is a dip in anisotropy due to maximal absorption by the ^1L_b state. Figure 5a shows such a characteristic dip around 285 nm in the excitation anisotropy spectrum of TOE. Thus, the sharp increase in anisotropy toward the red edge of the absorption
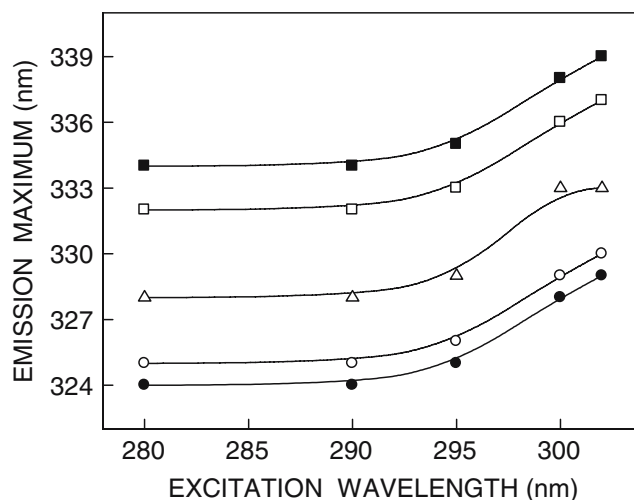

Fig. 3 Effect of changing excitation wavelength on the wavelength of maximum emission of TOE in AOT reverse micelles corresponding to w_o = 0 (*filled circle*), 5 (*open circle*), 10 (*open triangle*), 20 (*open square*), and 30 (*filled square*). The ratio of fluorophore (TOE) to surfactant (AOT) was 1:250 (mol/mol). See "Materials and methods" for other details

band is probably because the extent of depolarization in TOE is reduced at the red edge due to not only the decreased rotational rate of the fluorophore in the solvent-relaxed state, but also the photoselection of the predominantly ^1L_a transition, which in turn reduces the contribution to depolarization because of $^1L_b \rightarrow {}^1L_a$ equilibration.

For fluorophores incorporated in motionally restricted media, fluorescence anisotropy is also known to be dependent on emission wavelength. Under such conditions, a steady and significant decrease in anisotropy is observed with increasing emission wavelength (Mukherjee and Chattopadhyay 1995 and references therein). Figure 5b shows variation in steady-state anisotropy of TOE in AOT reverse micelles as a function of wavelength across its emission spectrum. As seen from the figure, there is a considerable reduction in anisotropy with increasing emission wavelength. The lowest anisotropy is observed toward the red edge where the solvent-relaxed emission predominates. Taken together, the changes in fluorescence anisotropy of TOE in AOT reverse micelles as a function of excitation and emission wavelengths reinforce the presence of motionally restricted environment in the vicinity of TOE.

Fluorescence lifetime serves as a faithful indicator of the local environment in which a given fluorophore is placed (Prendergast 1991). In addition, the fluorescence lifetime of tryptophan, in particular, is sensitive to solvent, temperature, and excited state interactions is well known (Kirby and Steiner 1970; Beechem and Brand 1985). A typical decay profile of the tryptophan moiety of TOE in AOT reverse micelles with its biexponential fitting and the various statistical parameters used to check the goodness of fit is shown in Fig. 6. The fluorescence lifetimes of TOE in AOT reverse micelles ob-
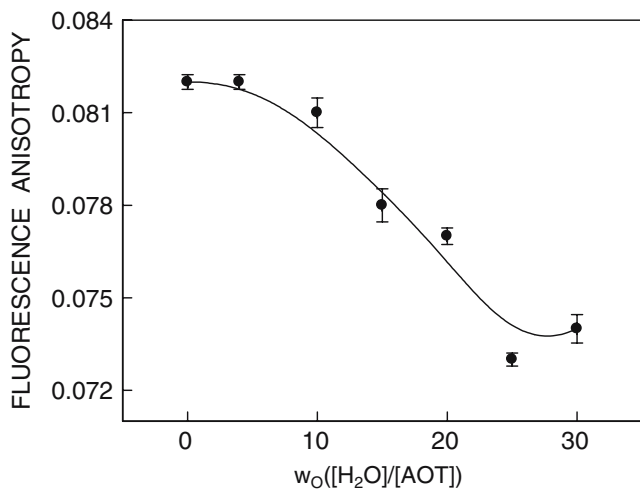
Fig. 4 Effect of increasing hydration on the fluorescence anisotropy of TOE in AOT reverse micelles. The excitation wavelength used was 280 nm and emission was monitored at 328 nm. The data points shown are the means ± standard errors of at least three independent measurements. All other conditions are as in Fig. 2. See "Materials and methods" for other details

Fig. 5 Fluorescence anisotropy of TOE in AOT reverse micelles corresponding to w_o = 0 (*filled circle*), 15 (*open circle*), and 30 (*filled square*) as a function of (**a**) excitation and (**b**) emission wavelength. The emission wavelength was 328 nm in all cases in (**a**), and the excitation wavelength was kept constant at 280 nm in all cases in (**b**). The data points shown are the means ± standard errors of at least three independent measurements. All other conditions are as in Fig. 2. See "Materials and methods" for other details

tained as a function of w_o are shown in Table 1. As seen from the table, all fluorescence decays could be fitted well with a biexponential function. We chose to use the mean fluorescence lifetime as an important parameter for describing the behavior of TOE in AOT reverse micelles since it is independent of the number of exponentials used to fit the time-resolved fluorescence decay. The mean fluorescence lifetimes of TOE in AOT reverse micelles calculated using Eq. 3 are plotted as a function of w_o (Fig. 7). In general, an increase in polarity of the tryptophan environment is known to reduce the lifetime of tryptophans due to fast deactivating processes in polar environments (Kirby and Steiner 1970). The increased polarity around the tryptophan moiety in AOT reverse micelles with increasing w_o is reflected in the decrease in the mean lifetime (~40%) of TOE with increase in the reverse micellar water content. Interestingly, the reduction in mean fluorescence lifetime is more pronounced at low values of w_o (up to w_o = 15).

To ensure that the observed change in steady-state anisotropy of TOE as a function of w_o (see Fig. 4) is not due to change in lifetime with increasing w_o (Fig. 7), the apparent (average) rotational correlation times for TOE in AOT reverse micelles with increasing w_o were calculated using Perrin's equation (Lakowicz 1999):

$$\tau_c = (<\tau> r)/(r_o - r) \qquad (4)$$

where r_o is the limiting anisotropy of tryptophan, r the steady-state anisotropy, and $<\tau>$ the mean fluorescence lifetime as calculated from Eq. 3. Although Perrin's equation is not strictly applicable to this system, it is assumed that this equation will apply to a first approximation, especially because we have used mean fluorescence lifetimes for the analysis of multiple
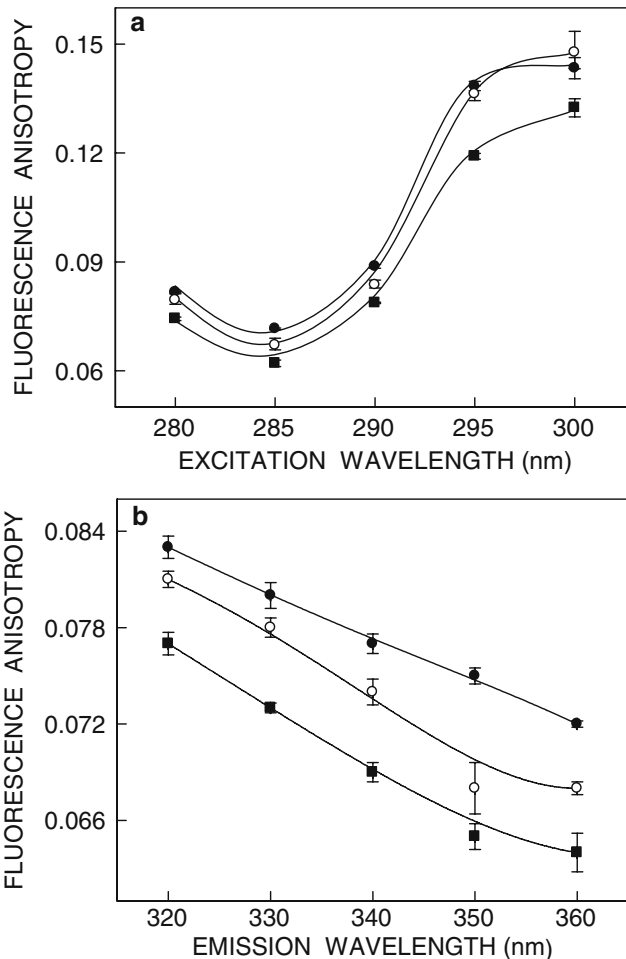
component lifetimes. The values of the apparent rotational correlation times, calculated this way using a value of r_o of 0.16 for excitation at 280 nm (Eftink et al. 1990), are shown in Fig. 7. The overall change in rotational correlation times of TOE with increasing w_o shows that the observed change in anisotropy values (Fig. 4) was not due to any lifetime-induced artifacts, and reinforces our earlier conclusion that there is a decrease in rotational restriction experienced by TOE with increasing hydration.

Discussion

Reverse micelles are relatively simple yet versatile systems and represent ideal systems to address a variety of
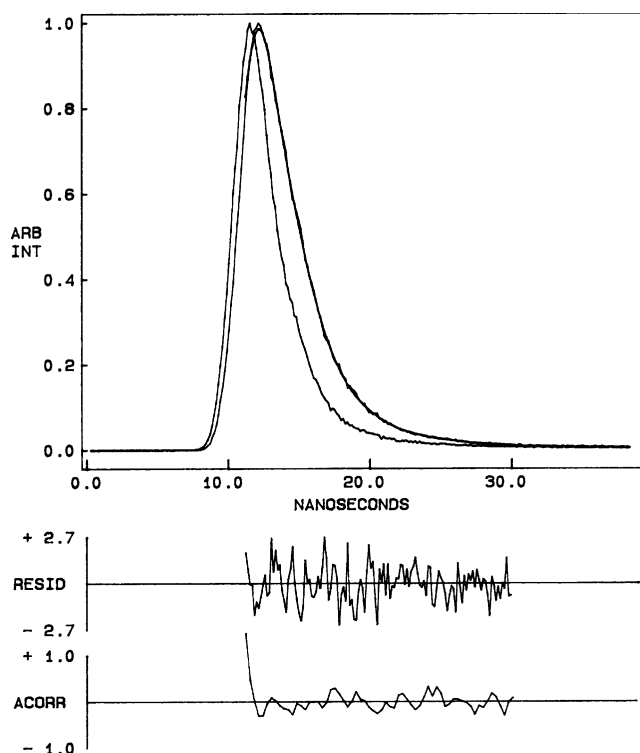
Fig. 6 Time-resolved fluorescence intensity decay of TOE in AOT reverse micelles at $w_o = 4$. Excitation wavelength was at 297 nm which corresponds to a peak in the spectral output of the nitrogen lamp. Emission was monitored at 328 nm. The sharp peak on the left is the lamp profile. The relatively broad peak on the right is the decay profile, fitted to a biexponential function. The two lower plots show the weighted residuals and the autocorrelation function of the weighted residuals. The ratio of fluorophore (TOE) to surfactant (AOT) was 1:500 (mol/mol). See "Materials and methods" for other details

problems in biology including their application as reaction media (Khmelnitsky et al. 1989; Carvalho and Cabral 2000) and in protein biotechnology (Melo et al. 2001). They offer certain inherent advantages in fluorescence studies over membranes since reverse micelles are smaller and optically transparent, have well-defined sizes, and are relatively scatter-free (Laane and Visser 1987; Visser et al. 1988). Reverse micelles represent a

Table 1 Lifetimes of TOE in AOT reverse micelles as a function of w_o

| [Water]/[surfactant] molar ratio[a] (w_o)	α_1	τ_1(ns)	α_2	τ_2(ns)
0	0.87	1.25	0.13	3.00
4	0.78	0.86	0.22	2.34
10	0.89	0.85	0.11	2.28
15	0.88	0.54	0.12	2.06
20	0.85	0.52	0.15	1.81
25	0.86	0.57	0.14	1.84
30	0.87	0.61	0.13	1.91

The excitation wavelength was 297 nm; emission was monitored at 328 nm [a]The ratio of TOE to AOT was 1:500 (mol/mol)

type of organized molecular assembly which offers the unique advantage of monitoring dynamics of molecules with varying states of hydration that is difficult to achieve with complex systems such as membranes. Hydration plays an important modulatory role in the formation and maintenance of organized molecular assemblies such as micelles, membranes, and folded proteins in aqueous solutions (Israelachvili and Wennerstörm 1996). Application of the wavelength-selective fluorescence approach to reverse micellar systems is therefore particularly appealing since REES is capable of monitoring the dynamics of the solvent molecules surrounding the fluorophore. In this paper, we have examined the effect of hydration on TOE, a model for tryptophan residues in membranes. We report here that TOE exhibits wavelength-selective fluorescence effects when bound to reverse micelles of AOT. Our results show that fluorescence parameters such as intensity, emission maximum, anisotropy, and lifetime of TOE in reverse micelles of AOT depend on [water]/[surfactant] molar ratio (w_o).

The ionization state of TOE under the conditions of our experiments and its consequence on our results deserve comment. The apparent pK_a of the amino group of TOE in water is ~ 9.7 (Chattopadhyay et al. 1997). The amino group of TOE would therefore predominantly be in the protonated state when bound to reverse micelles of AOT (see Fig. 1). Since AOT itself is negatively charged due to the sulfonate group, the restriction in the tryptophan environment of TOE could be partly due to the electrostatic interaction between these moieties. This could possibly account for the invariance of REES with w_o since the electrostatic interaction could somehow mask the effects of slow solvent reorientation. Interestingly, here we report REES for TOE in the so-called "dry micelles" ($w_o = 0$). However, the ternary phase diagram for AOT/water/nonpolar solvent shows that reverse micelles with $w_o = 0$ are not stable (Luisi and Magid 1986). Fortunately AOT always contains some water since it is impossible to obtain completely dry AOT.

The fluorescence decay of tryptophan in water is biexponential. This has been attributed to the rotamer model of tryptophan fluorescence, originally proposed by Szabo and Rayner (1980) and later confirmed by the analysis of conformational heterogeneity of tryptophan in crystals of erabutoxin b (Dahms et al. 1995). According to this model, the lifetime heterogeneity of tryptophan could be attributed to tryptophan rotamers that interconvert slowly in nanosecond time scale. These rotamers, defined relative to their C_α–C_β bond, have different distances between the carboxylate and amino groups, and the indole ring, and consequently exhibit different extents of electrostatic interactions between these groups. Since the fluorescence lifetime of indole is sensitive to the surrounding environment, different rotamers exhibit different lifetimes. The observation of short lifetimes is generally taken as an indication of extensive deactivation mechanism. Our lifetime analysis

Fig. 7 Effect of increasing amounts of water on mean fluorescence lifetime (*open circle*) of TOE in AOT reverse micelles. The excitation wavelength used was 297 nm and emission wavelength was set at 328 nm. Mean fluorescence lifetimes were calculated from Table 1 using Eq. 3. All other conditions are as in Fig. 6. See "Materials and methods" for other details. The apparent rotational correlation times (*filled circle*) of TOE in AOT reverse micelles are also shown. The apparent rotational correlation times are calculated using Eq. 4 (see text for other details)
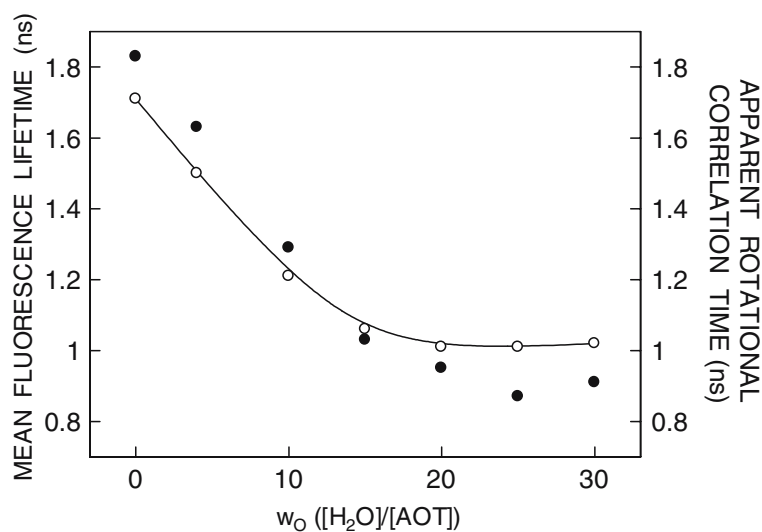
with TOE in AOT reverse micelles shows biexponential decays and a predominant short lifetime component, especially toward higher w_o values (see Table 1). We suggest that in the case of TOE, due to the esterification of the free carboxylic group of tryptophan by the octyl chain (which causes steric crowding) and the fact that the high hydrophobicity of this chain demands that it be embedded in the apolar region of the reverse micelle, it loses its freedom of rotation about the C_α–C_β bond. This is illustrated in Fig. 8 where the Newman projections of three rotamers along the C_α–C_β bond of TOE in its protonated form (the form predominant in AOT reverse micelles, see above) are shown. We propose that rotamer (a) will be preferred due to (1) lack of steric constraints between the octyl chain of TOE and the indole ring and (2) the stabilization gained from the energetically favorable electrostatic interaction between the delocalized π electron cloud of the indole ring and the positively charged quarternary nitrogen atom. This could represent a cation–π interaction which is known to be important in a number of interactions in biology (Dougherty 1996). Such interaction could lead to fluorescence quenching and reduction in fluorescence lifetime (Raghuraman and Chattopadhyay 2003). We further propose that the short lifetime component corresponds to rotamer (a). The predominance of the short lifetime component indicates that rotamer (a) has substantial contribution under such conditions because of energetically unfavorable steric crowding in rotamers (b) and (c). In other words, addition of the hydrophobic octyl chain to the tryptophan results in one of the rotamers (rotamer a) to be 'frozen' in space. Similar frozen rotamers are also expected in case of tryptophans that anchor transmembrane stretches of amino acids to the membrane interface, the hydrophobic transmembrane amino acid sequences acting as the orienting force in these cases. We must emphasize here that the model proposed here is a plausible one and alternate interpretations of our data cannot be ruled out at present.

It is known that the dynamics of liquids in confined spaces is different from that of their bulk counterparts (Granick 1991; Levinger 2002) and this constitutes one of the main reasons for the popularity that reverse micelles enjoy as a model system in studies of water dynamics. The highly structured, yet heterogeneous, water molecules in reverse micelles represent interesting models for water molecules present in biological systems such as membranes, which are more difficult to analyze experimentally. The properties of water in reverse micelles of AOT at low w_o values are rather different from those of bulk water (Jain et al. 1989; Ikushima et al. 1997; Brubach et al. 2001; Venables et al. 2001). Three types of water populations (pools) have been shown to coexist in reverse micelles. These are bound water, trapped water, and free water (Jain et al. 1989; Ikushima et al. 1997). The crucial parameter is the [water]/[surfactant] molar ratio which determines the relative proportions of these three types of water pools.

Water plays a crucial role in mediating lipid–protein interactions in membranes, thereby controlling the folding and functionality of membrane proteins (Ho and Stubbs 1992; Fischer et al. 1994; Sankararamakrishnan and Sansom 1995; Arumugam et al. 1996). For example, it has been previously shown using neutron diffraction of small peptides in membrane bilayers that there was a direct association of water with the peptides, possibly with a tryptophan residue (Jacobs and White 1989). It was suggested that such an effect, if enhanced by larger peptides, would be important for the insertion of helices into bilayers and for helix–helix interactions involving hydrogen bonding. Very recently, it has been shown that water molecules localized in the vicinity of highly conserved residues and in the retinal pocket of rhodopsin regulate the activity of rhodopsin and other G-protein-coupled receptors by mediating intermolecular interaction (Okada et al. 2002). Our results therefore could be potentially useful for the analysis of dynamics of proteins or peptides bound to

Fig. 8 Newman projections of three rotamers along the Cα–Cβ bond of TOE in its protonated form. See "Discussion" for details
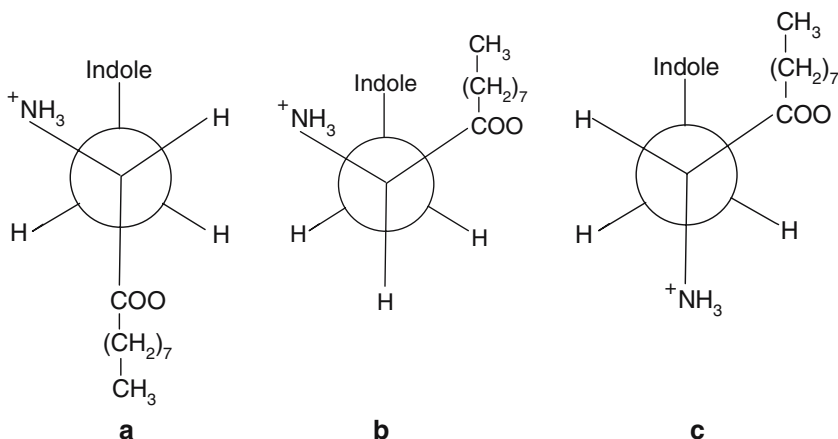
membranes or membrane-mimetic media under conditions of changing hydration.

References

Arumugam S, Pascal S, North CL, Hu W, Lee K-C, Cotten M, Ketcham RR, Xu F, Brenneman M, Kovacs F, Tian F, Wang A, Huo S, Cross TA (1996) Conformational trapping in a membrane environment: a regulatory mechanism for protein activity? Proc Natl Acad Sci USA 93:5872–5876

Becker MD, Greathouse DV, Koeppe RE, Andersen OS (1991) Amino acid sequence modulation of gramicidin channel function: effects of tryptophan-to-phenylalanine substitutions on the single-channel conductance and duration. Biochemistry 30:8830–8839

Beechem JM, Brand L (1985) Time-resolved fluorescence of proteins. Annu Rev Biochem 54:43–71

Bevington PR (1969) Data reduction and error analysis for the physical sciences. McGraw-Hill, New York

Bhattacharyya K (2003) Solvation dynamics and proton transfer in supramolecular assemblies. Acc Chem Res 36:95–101

Brubach J-B, Mermet A, Filabozzi A, Gerschel A, Lairez D, Krafft MP, Roy P (2001) Dependence of water dynamics upon confinement size. J Phys Chem B 105:430–435

Callis PR (1997) ^1L_a and ^1L_b transitions of tryptophan: applications of theory and experimental observations to fluorescence of proteins. Methods Enzymol 278:113–150

Carvalho CML, Cabral JMS (2000) Reverse micelles as reaction media for lipases. Biochimie 82:1063–1085

Chattopadhyay A (2003) Exploring membrane organization and dynamics by the wavelength-selective fluorescence approach. Chem Phys Lipids 122:3–17

Chattopadhyay A, Mukherjee S, Rukmini R, Rawat SS, Sudha S (1997) Ionization, partitioning, and dynamics of tryptophan octyl ester: implications for membrane-bound tryptophan residues. Biophys J 73:839–849

Chattopadhyay A, Mukherjee S, Raghuraman H (2002) Reverse micellar organization and dynamics: a wavelength-selective fluorescence approach. J Phys Chem B 106:13002–13009

Dahms TES, Willis KJ, Szabo AG (1995) Conformational heterogeneity of tryptophan in a protein crystal. J Am Chem Soc 117:2321–2326

Demmers JA, van Duijn E, Haverkamp J, Greathouse DV, Koeppe RE, Heck AJR, Killian JA (2001) Interfacial positioning and stability of transmembrane peptides in lipid bilayers studied by combining hydrogen/deuterium exchange and mass spectrometry. J Biol Chem 276:34501–34508

Dougherty DA (1996) Cation–pi interactions in chemistry and biology: a new view of benzene, Phe, Tyr, and Trp. Science 271:163–168

Eftink MR, Selvidge LA, Callis PR, Rehms AA (1990) Photophysics of indole derivatives: experimental resolution of L_a and L_b transitions and comparison with theory. J Phys Chem 94:3469–3479

Faeder J, Ladanyi BM (2000) Molecular dynamics simulations of the interior of aqueous reverse micelles. J Phys Chem B 104:1033–1046

Fischer WB, Sonar S, Marti T, Khorana HG, Rothschild KJ (1994) Detection of a water molecule in the active-site of bacteriorhodopsin: hydrogen bonding changes during the primary photoreaction. Biochemistry 33:12757–12762

de Foresta B, Gallay J, Sopkova J, Champeil P, Vincent M (1999) Tryptophan octyl ester in detergent micelles of dodecylmaltoside: fluorescence properties and quenching by brominated detergent analogs. Biophys J 77:3071–3084

Granick S (1991) Motions and relaxations of confined liquids. Science 253:1374–1379

Grinvald A, Steinberg IZ (1974) On the analysis of fluorescence decay kinetics by the method of least-squares. Anal Biochem 59:583–598

Ho C, Stubbs CD (1992) Hydration at the membrane protein–lipid interface. Biophys J 63:897–902

Ikushima Y, Saito N, Arai M (1997) The nature and structure of water/AOT/ethane (W/O) microemulsion under supercrititical conditions studied by high-pressure FT-IR spectroscopy. J Colloid Interface Sci 186:254–263

Israelachvili J, Wennerstörm H (1996) Role of hydration and water structure in biological and colloidal interactions. Nature 379:219–225

Jacobs RE, White SH (1989) The nature of the hydrophobic binding of small peptides at the bilayer interface: implications for the insertion of transbilayer helices. Biochemistry 28:3421–3437

Jain TK, Varshney M, Maitra A (1989) Structural studies of aerosol OT reverse micellar aggregates by FT-IR spectroscopy. J Phys Chem 93:7409–7416

Khmelnitsky YL, van Hoek A, Veeger C, Visser AJWG (1989) Detergentless microemulsions as media for enzymatic reactions. Spectroscopic and ultracentrifugation studies. J Phys Chem 93:872–878

Kirby EP, Steiner RF (1970) The influence of solvent and temperature upon the fluorescence of indole derivatives. J Phys Chem 74:4480–4490

Laane KVC, Visser AJWG (1987) Spectroscopy of reversed micelles. Photochem Photobiol 45:863–878

Ladokhin AS, Holloway PW (1995) Fluorescence of membrane-bound tryptophan octyl ester: a model for studying intrinsic fluorescence of protein–membrane interactions. Biophys J 69:506–517

Lakowicz JR (1999) Principles of fluorescence spectroscopy, 2nd edn. Plenum, New York

Lampert RA, Chewter LA, Phillips D, O'Connor DV, Roberts AJ, Meech SR (1983) Standards for nanosecond fluorescence decay time measurements. Anal Chem 55:68–73

Levinger NE (2002) Water in confinement. Science 298:1722–1723

Luisi PL, Magid LJ (1986) Solubilization of enzymes and nucleic acids in hydrocarbon micellar solutions. CRC Crit Rev Biochem 20:409–475

Melo EP, Aires-Barros MR, Cabral JMS (2001) Reverse micelles and protein biotechnology. Biotech Annu Rev 7:87–129

Miller AS, Falke JJ (2004) Side chains at the membrane–water interface modulate the signaling state of a transmembrane receptor. Biochemistry 43:1763–1770

Mukherjee S, Chattopadhyay A (1994) Motionally restricted tryptophan environments at the peptide–lipid interface of gramicidin channels. Biochemistry 33:5089–5097

Mukherjee S, Chattopadhyay A (1995) Wavelength-selective fluorescence as a novel tool to study organization and dynamics in complex biological systems. J Fluoresc 5:237–246

Mukherjee K, Moulik SP, Mukherjee DC (1993) Thermodynamics of micellization of aerosol OT in polar and nonpolar solvents. A calorimetric study. Langmuir 9:1727–1730

O'Connor DV, Phillips D (1984) Time-correlated single photon counting. Academic, London, pp 180–189

Okada T, Fujiyoshi Y, Silow M, Navarro J, Landau EM, Shichida Y (2002) Functional role of internal water molecules in rhodopsin revealed by x-ray crystallography. Proc Natl Acad Sci USA 99:5982–5987

Prendergast FG (1991) Time-resolved fluorescence techniques: methods and applications in biology. Curr Opin Struct Biol 1:1054–1059

Raghuraman H, Chattopadhyay A (2003) Organization and dynamics of melittin in environments of graded hydration: a fluorescence approach. Langmuir 19:10332–10341

Raghuraman H, Kelkar DA, Chattopadhyay A (2005) Novel insights into protein structure and dynamics utilizing the red edge excitation shift approach. In: Geddes CD, Lakowicz JR (eds) Reviews in fluorescence, vol 2. Springer, Berlin Heidelberg New York, pp 199–214

Reithmeier RAF (1995) Characterization and modeling of membrane proteins using sequence analysis. Curr Opin Struct Biol 5:491–500

Ruggiero AJ, Todd DC, Fleming GR (1990) Subpicosecond fluorescence anisotropy studies of tryptophan in water. J Am Chem Soc 112:1003–1014

Sankararamakrishnan R, Sansom MSP (1995) Water-mediated conformational transitions in nicotinic receptor M2 helix bundles: a molecular dynamics study. FEBS Lett 377:377–382

Schiffer M, Chang CH, Stevens FJ (1992) The functions of tryptophan residues in membrane proteins. Protein Eng 5:213–214

Sengupta B, Sengupta P (2000) Influence of reverse micellar environments on the fluorescence emission properties of tryptophan octyl ester. Biochem Biophys Res Commun 277:13–19

Szabo AG, Rayner DM (1980) Fluorescence decay of tryptophan conformers in aqueous solution. J Am Chem Soc 102:554–563

Ulmschneider MB, Sansom MSP (2001) Amino acid distributions in integral membrane protein structures. Biochim Biophys Acta 1512:1–14

Valeur B, Weber G (1977) Resolution of the fluorescence excitation spectrum of indole into the ^1L_a and ^1L_b excitation bands. Photochem Photobiol 25:441–444

Valeur B, Weber G (1978) A new red-edge effect in aromatic molecules: anomaly of apparent rotation revealed by fluorescence polarization. J Chem Phys 69:2393–2400

Venables DS, Huang K, Schmuttenmaer CA (2001) Effect of reverse micellar size on the librational band of confined water and methanol. J Phys Chem B 105:9132–9138

Visser AJWG, Vos K, van Hoek A, Santema JS (1988) Time-resolved fluorescence depolarization of Rhodamine B and Octadecylrhodamine B in triton X-100 micelles and aerosol OT reversed micelles. J Phys Chem 92:759–765

Zhou G-W, Li G-Z, Chen W-J (2002) Fourier transform infrared investigation on water states and the conformations of aerosol-OT in reverse microemulsions. Langmuir 18:4566–4571